Spin-parity analysis of the B meson*

S. U. Chung and S. D. Protopopescu
Brookhaven National Laboratory, Upton, New York 11973

G. R. Lynch, M. Alston-Garnjost, A. Barbaro-Galtieri, J. H. Friedman,†
R. L. Ott,‡ M. S. Rabin,§ and F. T. Solmitz
Lawrence Berkeley Laboratory, Berkeley, California 94720

S. M. Flatté
University of California, Santa Cruz, California 95060
(Received 9 October 1974)

We have done a J^P analysis of the low-mass $\pi^+\omega$ system, using the reaction $\pi^+p \to \pi^+\omega p$ at 7.1 GeV/c. We find that the B resonance cannot be $J^P = 0^-$ and must belong to the unnatural-parity series (1^+, 2^-, 3^+,...), regardless of the amount of interference between the B and the background. If we assume that the B does not interfere with the background, we find that all J^P states for the resonance are rejected except for 1^+. Even if interference effects are allowed in the analysis, a good fit with reasonable parameters is obtained only with the 1^+ hypothesis for the B meson. In an appendix, we give relevant theoretical formulas appropriate for a $\pi\omega$ system with any number of spin-parity states and arbitrary degrees of interference among them.

I. INTRODUCTION

The purpose of this paper is to present a fuller account of our spin-parity (J^P) analysis of the B region published in *Physics Letters*.[1] The spin-parity analysis of the B meson has in the past been performed under the assumption that the B region is in a pure spin-parity state and/or the resonance does not interfere with the background.[2] Our analysis presented here takes into account explicitly the interference effects among different spin-parity states. We have accomplished this by utilizing in the analysis certain symmetrized moments which are independent of opposite-parity interferences and by including in the theoretical formula only those interference effects resulting from like-parity states. In addition, the use of symmetrized moments made it possible to eliminate the non-negligible Δ^{++} events without introducing extraneous bias into the analysis. We have assumed, however, that the ω does not interfere with the background 3π system; in all the relevant moments studied we have found no evidence of the ω interfering with the background.

Data for this analysis come from a Berkeley Group A experiment on π^+p interactions at 7.1 GeV/c in the 82-in. hydrogen bubble chamber at SLAC. We have selected the ω events from 81 000 events of the reaction

$$\pi^+p \to \pi^+\pi^0\pi^-\pi^+p,$$

corresponding to about 42 events /μb statistics.[3] In Sec. II, we describe the selection of data for J^P analysis. In Sec. III we discuss what qualitative conclusions can be reached by a simple inspection of significant moments while in Sec. IV we give several of the more significant solutions from χ^2 fits to the moments. Density-matrix elements as a function to t' for the solution containing the J^P states 1^+, 1^-, and 0^- are given in Sec. V. Section VI has been reserved for summary and conclusions. In an Appendix, we give, in some detail, relevant theoretical formulas for the J^P analysis of a $\pi\omega$ system.

II. SELECTION OF DATA FOR χ^2 ANALYSIS

The 3π spectrum for events with $M(4\pi)<1.74$ GeV and $t'<1.0$ (GeV/c)^2 shows that the ω bump rides on a non-negligible (~20%) 3π background (see Fig. 1). It is important to eliminate this background since 3π events distributed according to phase space will simulate an s-wave 1^+ $\pi\omega$ state. The task is complicated by the fact that there are two possible 3π combinations. It is thus necessary to examine 6 interlacing bands formed by the ω region and two control regions on a scatter plot with the effective mass of one neutral 3π combination versus that of the other combination, as shown in Fig. 1. The ω region is defined by $0.760<M(3\pi)<0.805$ GeV; the control regions are defined by $0.69<M(3\pi)<0.735$ GeV and $0.830<M(3\pi)<0.875$ GeV. For the double-ω events, which are small in number (~5%), we have chosen for this analysis that 3π combination whose effective mass is closer to the accepted mass, i.e., 783 MeV. We performed a

background subtraction using the control regions, assuming that the background in the double-ω region (delineated by dotted lines in the insert to Fig. 1) can be approximated by the average of the four overlapping regions formed by the control bands (double-hatched regions in the insert). The background-subtraction procedure consisted of including the control-region events outside the overlapping bands with weight $w = -\frac{1}{2}$; the events from the 4 regions where the control bands overlap are used twice (once for each combination), with $w = -\frac{5}{8}$. Clearly events in the ω region have $w = 1$. These weights were used to modify the functions calculated for each event. Thus, the "weighted" unnormalized moments and their correlations are given by

$$H(lmLM) = \sum_i w_i h^{lm}_{LM}(\Omega^i, \Omega^i_1), \tag{1}$$

$$\delta H(lmLM)\delta H(l'm'L'M') = \sum_i w_i h^{lm}_{LM}(\Omega^i, \Omega^i_1) \times h^{l'm'}_{L'M'}(\Omega^i, \Omega^i_1), \tag{2}$$

where Ω stands for the decay angles of the B meson and Ω_1 stands for the decay angles of the ω meson (see Appendix), w_i is the afore-mentioned "weight" for the ith event, and $h^{lm}_{LM}(\Omega, \Omega_1)$ is given by a product of two D functions,

$$h^{lm}_{LM}(\Omega, \Omega_1) = D^{L}_{Mm}(\phi, \theta, 0)D^{l}_{m0}(\alpha, \beta, 0). \tag{3}$$

The procedure we have just described for eliminating non-ω 3π background assumes that there are no interferences between the ω and the 3π backgrounds contributing to the moments $H(lmLM)$. In the analysis described below, we use the moments with $l = 0$ or 2. It can be shown that no interference terms between different spin-parity states can contribute to the moments with $l = 0$; we thus assume that the 3π background under the ω has a negligible 1^- state. The moments with $l = 2$ can have contributions only from interference between 1^- and 3^- states; however, it is unlikely that there exists a substantial 3^- 3π state at the ω mass. Furthermore, all the moments with l up to 4 show no noticeable interference effects between the ω and the background.

In Figs. 2 and 3 we show the $\pi^+\omega$, π^+p, and ωp mass spectra, after non-ω background subtraction [$|t'| < 1.0$ (GeV/c)^2]. Clearly, there is still a strong source of background in the $\pi^+\omega$ system due to the copious production (~21%) of the $\Delta^{++}\omega$ channel. In order to eliminate this background, we have restricted the present analysis to those events with $\cos\theta < 0.8$ (in the helicity frame), which eliminated virtually all the $\Delta^{++}\omega$ events (see Fig. 4). To compensate for this cut we doubled the weight of all the events with $\cos\theta < -0.8$ (note that for those events which are used twice, only the combination with $\cos\theta < -0.8$ will have its weight doubled). It can be shown that if one uses the symmetrized moments (A32) and the data satisfy the following symmetry [see (A26b) and (A26a)]

$$I(\theta, \phi, \beta, \alpha) = I(\pi - \theta, \pi - \phi, \beta, \pi + \alpha), \tag{4}$$

$$I(\theta, \phi, \beta, \alpha) = I(\pi - \theta, \pi + \phi, \pi - \beta, -\alpha), \tag{5}$$

then the contribution to the moments from events with $\cos\theta > 0.8$ is identical to that for $\cos\theta < -0.8$. The first (second) formula results from parity conservation in the production (decay) of a $\pi\omega$

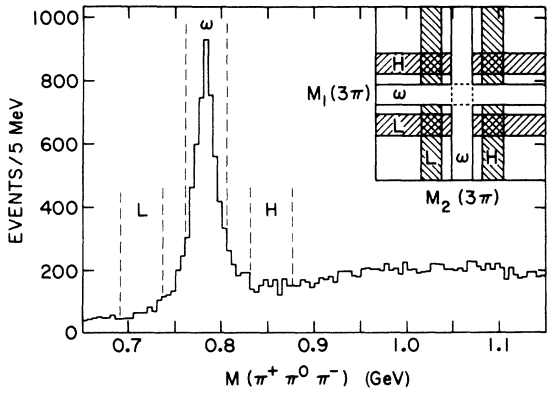

FIG. 1. $M(\pi^+\pi^-\pi^0)$ spectrum for $M(4\pi) < 1.74$ GeV and $t' < 1.0$ (GeV/c)^2. (Two combinations per event.) Insert shows the areas used for non-ω background subtraction. Regions L, ω, and H correspond, respectively, to 0.69–0.735 GeV, 0.760–0.805 GeV, and 0.830–0.875 GeV.

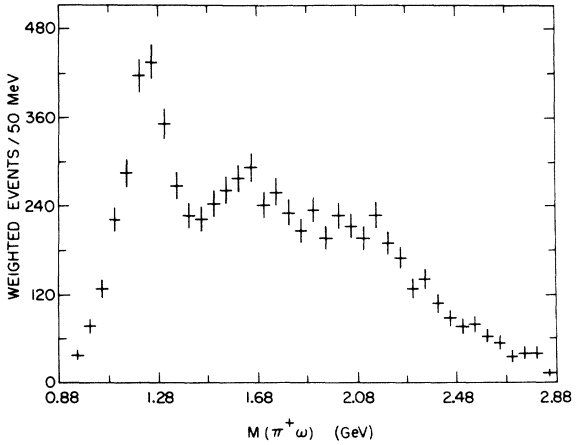

FIG. 2. $M(\pi^+\omega)$ spectrum for $t' < 1.0$ (GeV/c)^2 after non-ω background subtraction.

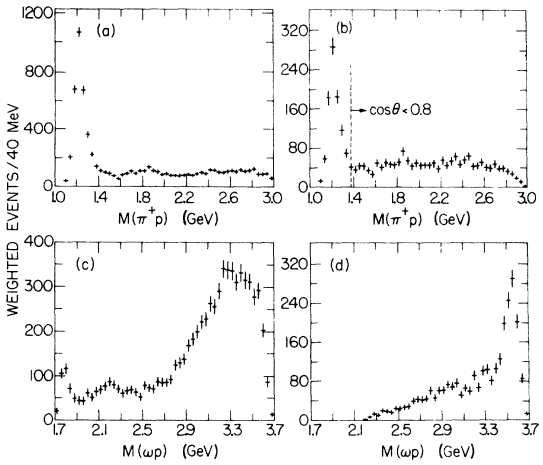

FIG. 3. (a) $M(\pi^+p)$ spectrum for $t'<1.0$ GeV/c^2 after non-ω background subtraction. (b) Same as (a) for $M(\pi^+\omega)<1.48$ GeV. Dashed line corresponds to $\cos\theta = 0.8$ for $M(\pi^+\omega)=1.25$ GeV. (c) $M(\omega p)$ spectrum with same cuts as (a). (d) $M(\omega p)$ spectrum with same cuts as (b).

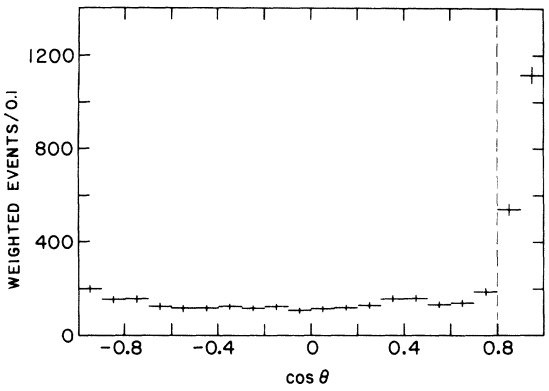

FIG. 4. Distribution in $\cos\theta$ with non-ω background subtraction. Dashed line indicates the cut done to remove Δ^{++} events.

system, if one assumes that interferences between opposite parity states are absent. In order to see if the data satisfy the symmetry (4),(5), we divided the subsample of events with $-0.8<\cos\theta<+0.8$ into a number of four-dimensional cells (in the space defined by Ω and Ω_1) and checked for the difference between a given cell and that related via symmetry (4),(5). We have obtained a χ^2 of 24 for 16 degrees of freedom (for 32 cells), indicating that our data indeed satisfy the symmetry. We have also done this check for various mass and $|t'|$ cuts; in all cases the symmetry was well satisfied. However, we should emphasize that the absence of interferences between opposite parity states is only approximately true; with statistics higher than ours one may no longer be able to ignore the interference effects.

III. CONVENTIONAL MOMENT ANALYSIS

If the B does not interfere with the background $\pi\omega$ system, it is possible by a simple background-subtraction method to measure all the independent experimentally measurable moments. In particular, the following combinations of moments [see Eqs. (A40a), (A40b), and (A45)] are useful for J^P determination (L = even ≥ 2):

$$H(0000)+5H(2000)=N\langle\tfrac{3}{2}(5\cos^2\beta-1)\rangle=3N|F_0|^2, \quad (6)$$

$$H(0000)-\tfrac{5}{2}H(2000)=N\langle\tfrac{3}{4}(3-5\cos^2\beta)\rangle=3N|F_1|^2, \quad (7)$$

$$\Delta_{JP}(LM)\equiv\left[\frac{2L(L+1)}{3(L-1)(L+2)}\right]^{1/2}[H(00LM)-\tfrac{5}{2}H(20LM)]$$
$$-P(-)^{J-1}\left[1-\frac{L(L+1)}{2J(J+1)}\right]5H(22LM). \quad (8)$$

(Here P is the intrinsic parity of the resonance.) If the resonance is in state J^P, the quantity given in (8) should be identically zero regardless of the production mechanism. Use of these moments leads to a unique determination of the spin parity for the B meson. Note that $\Delta_{JP}(2M)$ cannot distinguish between the states 1^+ and 2^+ or 1^- and 2^-; note also that if $J=1$, then all H's with $L>2$ are zero.

We display in Fig. 5 the unnormalized moments up to $L=2$ that are significant from the point of view of J^P determination. None of the moments with $L\geq 3$ have statistically significant deviations from zero in the B region, indicating that spins greater than 1 are not required to describe the bump. We can go far in deducing the spin-parity state of the B by a mere examination of the moments displayed: (1) The combination of moments [shown in Fig. 5(c)], which is proportional to $|F_1|^2$, has a significant deviation from background in the B region, indicating that the B cannot have $J^P=0^-$ ($F_1=0$ if $J=0$). (2) The moment shown in Fig. 5(b), which is proportional to $|F_0|^2$, deviates significantly ($\sim 3\sigma$ effect) in the B region as well; this shows that the B belongs to the unnatural spin-parity series, i.e., $J^P=1^+$, 2^-, 3^+, etc. ($F_0=0$ for natural spin-parity series). (3) In addition, the moments Δ_1-(20) and Δ_2-(20), shown in Figs. 5(d) and 5(e), indicate that the resonance is consistent with being in states 1^+ or 2^+ but not in states 1^- or 2^-. All other $\Delta_{JP}(20)$ for unnatural parity (not shown) have the same significant structure as Δ_2-(20) indicating that the data reject all

unnatural-parity series except 1^+. (4) That we see no significant moment with $L \geq 3$ indicates that spins greater than 1 are *not required* by the data. From these observations, it emerges that $J^P = 1^+$ is the only possible hypothesis for the B meson, if we assume the resonance does not interfere with background. We emphasize that remarks (1) and (2) are not affected by the presence of interference effects; they depend only on the assumption that the B bump consists of a single object with a given spin parity. In order to be more quantitative, we have done χ^2 fits which we describe in Sec. IV.

IV. DESCRIPTION OF FITS

We have done χ^2 fits to the moments (including correlations) for $M(\pi^+\omega) < 1.48$ GeV and $|t'| < 1.0$ $(\mathrm{GeV}/c)^2$. The data were divided into 5 mass bins; the first bin was for $M(\pi^+\omega)$ between 0.92 GeV and 1.08 GeV, the other four were 100 MeV each. We shall refer to the 3 bins between 1.08 GeV and 1.38 GeV as the B region. The free parameters in the fits were the number of events for each partial wave $[N(J^P)]$, the density-matrix elements $\rho^{J^P J^{P'}}_{m\,m'}$ and the decay amplitudes $F^{J^P}_\lambda$ [see Eqs. (A5)–(A8)]. For the final fits presented in this paper we have assumed that the density-matrix elements (excepting the interference terms) and the decay amplitudes $F^{J^P}_\lambda$ do not vary as a function of mass in the B region. We found by allowing those parameters to vary as a function of mass that the results were compatible with this assumption and, furthermore, there was no significant improvement in χ^2.

We should note that, if the $\pi\omega$ system is sufficiently complex, it is not in general possible to determine the spin-parity uniquely, for the number of parameters exceeds that of the measurable moments. We have therefore limited the number of partial waves in each fit to three or less. We will describe in detail only the most significant solutions.

A. $1^+1^-0^-$ fit

Because we use the symmetrized moments (see appendix) it is not necessary to consider the interference between 1^+ and 1^- nor 1^+ and 0^-. The interference term between 1^- and 0^- contributes only to one moment: $H(2111)$ (which is consistent with zero throughout). If the 1^+ state comes from a pure resonance, then F_0 and F_1 are relatively real. In this case, this moment has no contribution from the 1^+ state, so we left it out of the analysis. We therefore included for each mass bin 14 moments, which are given for the B region in Table I, while we had 10 free parameters,

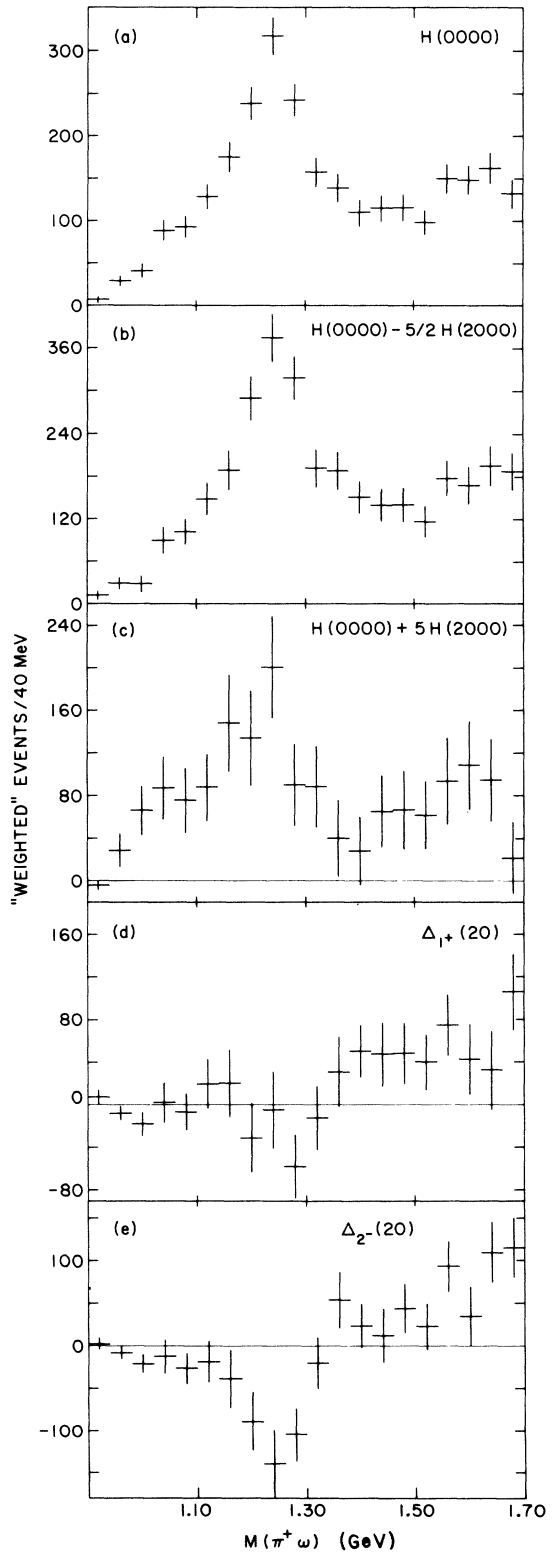

FIG. 5. Moments as functions of $M(\pi^+\omega)$ for $t' < 1.0$ $(\mathrm{GeV}/c)^2$ with non-ω background subtraction and after compensating for Δ^{++} cut: (a) $H(0000) = M(\pi^+\omega)$ spectrum; (b) $H(0000) + 5H(2000) = N\langle \frac{3}{2}(5\cos^2\beta - 1)\rangle$; (c) $H(0000) - \frac{5}{2} H(2000) = N\langle \frac{3}{4}(3 - 5\cos^2\beta)\rangle$; (d) Δ_1+(20), Δ_2-(20).

TABLE I. Experimental and predicted moments.

Moments	Experimental	Theory $1^+1^-0^-$	Theory $2^-1^-0^-$	Theory $2^+1^+0^-$	Moments	Experimental	Theory $1^+1^-0^-$	Theory $2^-1^-0^-$	Theory $2^+1^+0^-$
	(a) $1.08 < M(\pi^+\omega) < 1.18$ GeV					(b) $1.18 < M(\pi^+\omega) < 1.28$ GeV			
$H(0000)$	352 ± 24				$H(0000)$	672 ± 32			
$H(0020)$	6 ± 13	−10	3	−1.9	$H(0020)$	-49 ± 15	−20	−46	−28
$H(0021)$	7 ± 7	−5	14	4.3	$H(0021)$	-1 ± 10	−9	8	−8
$H(0022)$	2 ± 7	−5	0.5	3.1	$H(0022)$	-15 ± 9	−7	−17	−19
$5H(2000)$	-44 ± 56	−69	−85	−108.6	$5H(2000)$	-271 ± 68	−266	−305	−358
$5H(2020)$	33 ± 31	28	−7	1.9	$5H(2020)$	64 ± 33	53	42	28
$5H(2021)$	31 ± 17	14	17	−4.3	$5H(2021)$	47 ± 22	26	19	8
$5H(2022)$	21 ± 14	14	20	−3.1	$5H(2022)$	22 ± 20	24	32	19
$5H(2120)$	20 ± 17	29	8	0	$5H(2120)$	14 ± 23	54	14	0
$5H(2121)$	17 ± 13	15	19	0	$5H(2121)$	39 ± 15	23	39	0
$5H(2122)$	14 ± 11	15	17	0	$5H(2122)$	32 ± 15	27	31	0
$5H(2220)$	52 ± 16	48	66	35.0	$5H(2220)$	108 ± 23	84	105	85
$5H(2221)$	32 ± 11	24	11	24.0	$5H(2221)$	13 ± 16	44	−3	23
$5H(2222)$	37 ± 15	24	6	36.1	$5H(2222)$	38 ± 17	52	47	56
$H(0040)$	16 ± 8	0	0.4	−3.0	$H(0040)$	-8 ± 10	0	5	−13
$H(0041)$	-3 ± 6	0	−0.2	−0.8	$H(0041)$	-12 ± 8	0	−3	−3
$H(0042)$	-3 ± 6	0	0.5	0.6	$H(0042)$	7 ± 7	0	6	2
$H(0043)$	-2 ± 5	0	0	0.7	$H(0043)$	-9 ± 7	0	0	3
$H(0044)$	-9 ± 5	0	0	0	$H(0044)$	-1 ± 7	0	0	0
$5H(2040)$	11 ± 21	0	−3	3.1	$5H(2040)$	-44 ± 22	0	−7	13
$5H(2041)$	15 ± 16	0	1	0.8	$5H(2041)$	19 ± 18	0	4	3
$5H(2042)$	-23 ± 13	0	−3	−0.6	$5H(2042)$	-18 ± 16	0	−8	−2
$5H(2043)$	2 ± 11	0	0	−0.7	$5H(2043)$	-29 ± 15	0	0	−3
$5H(2044)$	11 ± 11	0	0	0	$5H(2044)$	3 ± 15	0	0	0
$5H(2140)$	2 ± 14	0	−3	0	$5H(2140)$	19 ± 18	0	−5	0
$5H(2141)$	-8 ± 9	0	1	0	$5H(2141)$	-11 ± 11	0	3	0
$5H(2142)$	3 ± 9	0	−3	0	$5H(2142)$	-6 ± 12	0	−6	0
$5H(2143)$	5 ± 8	0	0	0	$5H(2143)$	5 ± 11	0	0	0
$5H(2144)$	12 ± 8	0	0	0	$5H(2144)$	-1 ± 10	0	0	0
$5H(2240)$	-5 ± 13	0	−2	−5.9	$5H(2240)$	-30 ± 17	0	−11	−25
$5H(2241)$	-3 ± 9	0	1	−1.5	$5H(2241)$	6 ± 12	0	6	−6
$5H(2242)$	-2 ± 10	0	−3	1.1	$5H(2242)$	-7 ± 13	0	−13	5
$5H(2243)$	-9 ± 9	0	0	1.3	$5H(2243)$	27 ± 12	0	0	6
$5H(2244)$	6 ± 9	0	0	0	$5H(2244)$	-5 ± 12	0	0	0
$5H(2111)$	-13 ± 17	0	0	0	$5H(2111)$	-7 ± 21	0	0	0
$5H(2131)$	-7 ± 10	0	0	0	$5H(2131)$	-7 ± 13	0	0	0
$5H(2132)$	-1 ± 10	0	−2	0	$5H(2132)$	-16 ± 13	0	−4	0
$5H(2133)$	6 ± 9	0	0	0	$5H(2133)$	16 ± 13	0	0	0
$5H(2231)$	-2 ± 10	0	0	0	$5H(2231)$	-22 ± 14	0	0	0
$5H(2232)$	8 ± 11	0	−4	0	$5H(2232)$	-29 ± 15	0	−20	0
$5H(2233)$	-14 ± 10	0	0	0	$5H(2233)$	-15 ± 13	0	0	0

namely $N(1^+)$, ρ_{11}, ρ_{1-1}, $\mathrm{Re}\rho_{10}$, and F_1 for 1^+, $N(1^-)$, ρ_{11}, ρ_{1-1}, and $\mathrm{Re}\rho_{10}$ for 1^-, and $N(0^-)$ for 0^-. Thus the system is over-constrained. We have found further that the density elements for 1^+ and 1^-, and $F_1^{1^+}$ do not vary significantly in the B region (1.08–1.38 GeV); so we have fitted those three regions simultaneously assuming no variation in those parameters as a function of mass. We have also found that it is not necessary to include a phase between F_1 and F_0; no significant improvement in the fit results from varying the phase.

The fit we obtained is quite good [$\chi^2 = 48.1$ for 34 degrees of freedom, CL (confidence level) ~6%]; in particular in the B region we have $\chi^2 = 32$ for 26 degrees of freedom, CL ~19%. The parameters for this fit are given in Tables II and III and the number of events for each partial wave is given in Fig. 6. One can see a clear resonance with $J^P = 1^+$ at the B mass, a smooth $J^P = 1^-$, and

TABLE I. *(Continued)*

Moments	Experimental	Theory $1^+1^-0^-$	Theory $2^-1^-0^-$	Theory $2^+1^+0^-$
	(c) $1.28 < M(\pi^+\omega) < 1.38$ GeV			
$H(0000)$	422 ± 27			
$H(0020)$	8 ± 14	-12	20	-9
$H(0021)$	-3 ± 9	-4	0.3	2
$H(0022)$	-1 ± 7	5	-6	-2
$5H(2000)$	-269 ± 59	-298	-306	-305
$5H(2020)$	43 ± 32	25	-20	9
$5H(2021)$	20 ± 18	10	4	-2
$5H(2022)$	18 ± 15	1	7	2
$5H(2120)$	17 ± 18	20	-4	0
$5H(2121)$	15 ± 14	10	12	0
$5H(2122)$	-1 ± 11	10	4	0
$5H(2220)$	4 ± 18	17	19	52
$5H(2221)$	20 ± 13	14	-3	28
$5H(2222)$	60 ± 17	42	24	46
$H(0040)$	-3 ± 10	0	4	-5
$H(0041)$	3 ± 7	0	-2	-2
$H(0042)$	0 ± 7	0	5	1
$H(0043)$	2 ± 5	0	0	1
$H(0044)$	-5 ± 5	0	0	0
$5H(2040)$	-13 ± 23	0	-4	6
$5H(2041)$	-10 ± 15	0	2	1.5
$5H(2042)$	-7 ± 14	0	-5	-1
$5H(2043)$	20 ± 11	0	0	-1.3
$5H(2044)$	1 ± 11	0	0	0
$5H(2140)$	-8 ± 14	0	-2	0
$5H(2141)$	9 ± 10	0	1	0
$5H(2142)$	0 ± 9	0	-2	0
$5H(2143)$	3 ± 9	0	0	0
$5H(2144)$	14 ± 8	0	0	0
$5H(2240)$	-30 ± 16	0	-8	-11
$5H(2241)$	-24 ± 11	0	4	-3
$5H(2242)$	9 ± 11	0	-10	2
$5H(2243)$	4 ± 12	0	0	3
$5H(2244)$	-15 ± 9	0	0	0
$5H(2111)$	-21 ± 18	0	0	0
$5H(2131)$	6 ± 12	0	0	0
$5H(2132)$	-7 ± 10	0	-1	0
$5H(2133)$	4 ± 9	0	0	0
$5H(2231)$	-19 ± 12	0	0	0
$5H(2232)$	-4 ± 13	0	-7	0
$5H(2233)$	-12 ± 12	0	0	0

Moments	$0.90 < M(\pi^+\omega) < 1.08$ GeV Experiment	$1^+1^-0^-$	$1.38 < M(\pi^+\omega) < 1.48$ GeV Experiment	$1^+1^-0^-$
	(d) Fits to bins adjacent to the B region [a]; 5 degrees of freedom			
$H(0000)$	207 ± 18		278 ± 23	
$H(0020)$	-5 ± 8	2	50 ± 13	38
$H(0021)$	-5 ± 6	-4	16 ± 7	9
$H(0022)$	-7 ± 5	-5	3 ± 6	9
$5H(2000)$	-26 ± 40	-38	-110 ± 51	-82
$5H(2020)$	20 ± 19	-6	27 ± 31	33
$5H(2021)$	33 ± 13	27	9 ± 16	14
$5H(2022)$	4 ± 11	5	-6 ± 11	-6
$5H(2120)$	-29 ± 13	-4	-8 ± 17	-3
$5H(2121)$	22 ± 9	24	5 ± 13	-1
$5H(2122)$	-4 ± 9	0	-12 ± 10	0
$5H(2220)$	17 ± 12	3	36 ± 13	42
$5H(2221)$	14 ± 9	14	-5 ± 10	3
$5H(2222)$	-12 ± 9	-14	35 ± 14	25
	$\chi^2 = 9.7$		$\chi^2 = 6.7$	

[a] Only $1^+1^-0^-$ fits to these regions are given.

a small $J^P = 0^-$ background throughout the B region. The fitted decay parameters for the 1^+ state indicate that although the D-wave orbital angular momentum is small (~4%), it is significantly nonzero and interferes strongly with the S wave ($|D/S| = 0.21 \pm 0.08$ in the B region). From the density-matrix elements it appears that the 1^+ state is produced mainly via natural-parity exchange. A more detailed study of the production of these states will be given in Sec. IV.

B. $2^+1^-0^-$ fit

For this fit and the next we will only present results for the B region. As in the previous case we do not need to consider the interference between 2^+ and 1^- or 2^+ and 0^-. The moments with $L \geq 3$ are consistent with zero in the B region, which indicates that spins greater than 1 are not necessary to explain the data; we do, however, have to include them explicitly for this fit. We

TABLE II. Results of $(1^+1^-0^-)$ fit ($\chi^2 = 48.1$, number of degrees of freedom = 34, CL ~ 6%).

Mass bin (GeV)	F_1	$N(1^+)$ [a]	$N(1^-)$ [a]	$N(0^-)$ [a]
0.90–1.08	0.58 ± 0.05	155 ± 38	46 ± 20	6 ± 25
1.08–1.18 [b]	0.65 ± 0.02 [c]	307 ± 50	0 ± 50	46 ± 48
1.18–1.28 [b]	0.65 ± 0.02 [c]	570 ± 120	56 ± 114	44 ± 33
1.28–1.38 [b]	0.65 ± 0.02 [c]	215 ± 89	200 ± 81	6 ± 22
1.38–1.48	−0.04 ± 0.34	66 ± 24	212 ± 55	0 ± 25

[a] $N(J^P)$ denotes the number of events in J^P state.

[b] F_1 and $\rho_{mm'}$ (for 1^+ and 1^-) are assumed constant in the $M(\pi^+\omega)$ region 1.08 to 1.38 GeV; no appreciable improvement in the χ^2 fit results by varying these from region to region. The density-matrix elements for the 1^+ state are $\rho_{11} = 0.23 \pm 0.02$, $\rho_{1-1} = -0.13 \pm 0.03$, and $\mathrm{Re}\rho_{10} = 0.09 \pm 0.02$; those of the 1^- state are $\rho_{11} = 0.29 \pm 0.06$, $\rho_{1-1} = 0.17 \pm 0.10$, and $\mathrm{Re}\rho_{10} = 0.01 \pm 0.05$. Both are calculated in the s-channel helicity frame.

[c] This corresponds to $|D/S| = 0.21 \pm 0.08$.

therefore included 41 moments at each mass bin, which are given in parts (a)–(c) of Table I. As in the previous fit we have assumed that the density-matrix elements (there are no decay parameters in this case) do not vary as a function of mass. There are, therefore, a total of 20 parameters for 123 points, i.e., 11 density-matrix elements (8 for 2^+ and 3 for 1^-), and 3 normalization parameters at each mass bin [$N(2^+)$, $N(1^-)$, and $N(0^-)$]. Again, we do not include the 1^-0^- interference term, i.e., $H(2111)$. Some of the 2^+ density-matrix elements were found to be consistent with zero, and since the χ^2 did not change significantly when they were set to zero, they have been fixed at that value for the final fit. Tables III and IV give the values of the parameters for the best fit we could obtain, which has $\chi^2 = 146$ for 105 degrees of freedom [$P(\chi^2) = 0.6\%$]. This fit is thus rather poor. Furthermore, for the 2^+ state $\rho_{22} = 0.31 \pm 0.03$, which is rather unusual for a peripheral spin-2 resonance production. For all these reasons, this fit must be considered definitely unsatisfactory, and to that extent we claim that 2^+ assignment for the B meson is ruled out.

C. $2^-1^-0^-$ fit

For this fit interference effects between 2^-, 1^-, and 0^- cannot be neglected. We again include 41 moments for each mass bin, while the total number of possible parameters at each mass is 27; 8 $\rho_{m\,m'}$ for 2^-, 3 $\rho_{m\,m'}$ for 1^-, 7 interference density-matrix elements for 1^-2^-, 3 for 2^-0^-, 1 interference term for 1^-0^-, 3 normalizations [$N(2^-)$, $N(1^-)$, $N(0^-)$], and $F_1^{2^-}$. Many of these parameters turn out to be consistent with zero and do not add anything to the fit, so they were fixed to zero. Also, the noninterference density-matrix elements were assumed constant as a function of mass. So for the final fit we used 29 parameters (out of a possible total of 81) for 123 points. The χ^2 for this fit is 128 for 94 degrees of freedom, which is marginal [$P(\chi^2) = 1\%$]. The parameters of the fit are given in Tables III, IV, and V. Clearly the data can accommodate a 2^- resonance with smooth, relatively large 1^- and 0^- background states. Note that the fit requires strong interference between 2^- and 1^-, and 2^- and 0^-; i.e., the interference density-matrix elements are large and significantly nonzero.

TABLE III. Density-matrix elements for 3 fits in the B region.

Fit	State	ρ_{11}	ρ_{1-1} [a]	$\mathrm{Re}\rho_{10}$ [a]	ρ_{22}	$\mathrm{Re}\rho_{21}$	$\mathrm{Re}\rho_{20}$	$\mathrm{Re}\rho_{2-1}$ [a]	ρ_{2-2} [a]
$1^+1^-0^-$	1^+	0.23 ± 0.02	−0.13 ± 0.03	0.09 ± 0.02					
	1^-	0.29 ± 0.06	0.17 ± 0.10	0.01 ± 0.05					
$2^+1^-0^-$	2^+	0.11 ± 0.02	0.09 ± 0.03	0	0.31 ± 0.03	−0.04 ± 0.02	0.06 ± 0.02	0.02 ± 0.02	0
	1^-	0.23 ± 0.06	0.39 ± 0.10	−0.13 ± 0.05					
$2^-1^-0^-$	2^-	0.21 ± 0.04	0	0	0.25 ± 0.03	−0.08 ± 0.13	−0.10 ± 0.06	0	0
	1^-	0.49 ± 0.07	−0.03 ± 0.10	−0.07 ± 0.07					

[a] Whenever these parameters were found to be consistent with zero within less than one standard deviation, they were fixed to zero.

The density-matrix elements of 2^- and 1^- indicate that equal amounts of natural- and unnatural-parity exchange would be required to describe their production (i.e., ρ_{11} is significantly non-zero while ρ_{1-1} is consistent with zero). Furthermore, ρ_{22} is large ($\rho_{22} = 0.25 \pm 0.02$), indicating that the 2^- spin state must be produced strongly aligned to the helicity direction (a ρ_{22} as large as this has never been observed in the production of spin-2 resonances). We have looked at the eigenvalues of the full density matrix (which includes the interference density-matrix elements) to check if the solution satisfies positivity constraints. We found that one of the eigenvalues is negative, but the violation is small, slightly more than one standard deviation. This raises the possibility that with higher statistics one may be able to rule out this solution.

Although from the density-matrix elements one may find this solution artificial and unsatisfactory, it is clearly not possible with the present data to rule it out by purely "kinematical" considerations.

V. DENSITY MATRIX AS A FUNCTION OF t'

Assuming that the solution with 1^+, 1^-, and 0^- partial wave is the correct one, we have studied the variation of the density matrix as a function of t' in the B region. We have taken the events with $1.08 < M(\pi^+\omega) < 1.38$ GeV and divided them into three t' bins: $t' < 0.1$ (GeV/c)^2, $0.1 < t' < 0.4$ (GeV/c)^2, and $0.4 < t' < 1.0$ (GeV/c)^2. At each t' bin we repeated the fit described in Sec. IV A but kept F_1 fixed at the values obtained previously, since, if final-state interactions can be neglected, it should not vary as a function of t. The results are given in Tables VI and VII and in Figs. 7 and 8. They show that the 1^+ state is strongly peaked at low t' [the slope $\approx 5.5 \pm 1.8$ (GeV/c)$^{-2}$], but there is no apparent dip for either the 1^+ or 1^- state.

We found solutions with high probability for $t' < 0.1$ (GeV/c)^2 and $0.1 < t' < 0.4$ (GeV/c)^2; however, for $0.4 < t' < 1.0$ (GeV/c)^2 the fit is rather poor [$P(\chi^2) = 0.5\%$]. If we allow F_1 to vary in that bin, the fit does not improve substantially, but if we also allow a phase between F_1 and F_0, a barely acceptable fit can be obtained [$P(\chi^2) = 1\%$]. A better fit can also be obtained if we introduce small amounts of higher-spin states. The low

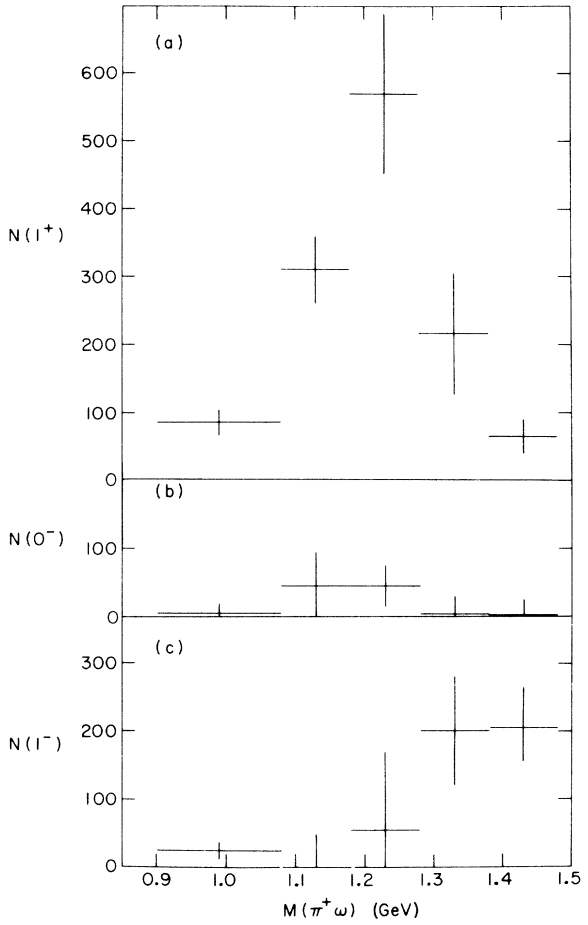

FIG. 6. Number of events in each J^P state [$N(J^P)$] as function of $M(\pi^+\omega)$ found by a fit to the data assuming that only 1^+, 1^-, and 0^- waves are significant.

TABLE IV. Results of $2^+1^-0^-$ and $2^-1^-0^-$ fits.

Mass bin (GeV)	$2^+1^-0^-$ fit $N(2^+)$	$N(1^-)$	$N(0^-)$	F_1 [a]	$2^-1^-0^-$ fit $N(2^-)$	$N(1^-)$	$N(0^-)$
1.08–1.18	137 ± 32	137 ± 37	80 ± 18	0.68 ± 0.03 [b]	83 ± 40	205 ± 40	64 ± 50
1.18–1.28	564 ± 65	0 ± 65	107 ± 20	0.68 ± 0.03	318 ± 80	254 ± 70	100 ± 50
1.28–1.38	280 ± 77	131 ± 77	38 ± 20	0.68 ± 0.03	215 ± 40	172 ± 40	35 ± 20

[a] F_1 was found to be the same in all 3 mass bins.
[b] This corresponds to $|F/P| = 0.44 \pm 0.18$.

TABLE V. $2^-1^-0^-$ fit interference terms.[a]

Mass bin (GeV)	ρ_{11}^{21}	ρ_{20}^{21}	ρ_{10}^{20}	ρ_{20}^{20}
1.08–1.18	−0.08 ± 0.05	0.06 ± 0.04	0.33 ± 0.12	0.15 ± 0.11
1.18–1.28	−0.14 ± 0.03	0.11 ± 0.03	0.23 ± 0.09	0.08 ± 0.08
1.28–1.38	0.03 ± 0.03	0.06 ± 0.03	0.15 ± 0.17	0.01 ± 0.11

[a] All other interference terms were found consistent with zero and therefore were fixed at zero.

probability for the fit given in Table VI may therefore indicate that our assumptions break down for $0.4<t'<1.0$ $(\mathrm{GeV}/c)^2$. However, with the present level of statistics it is not possible to distinguish between the various possibilities, i.e., whether we must include effects of final-state interactions.

The values obtained for the density-matrix elements indicate that the 1^+ state is produced mainly via natural-parity exchange such as ω exchange; for example, $\rho_{11}+\rho_{1-1}$ is small for the 1^+ state, while the opposite holds for $\rho_{11}-\rho_{1-1}$. In contrast, the 1^- state is produced by both natural- and unnatural-parity exchanges.

VI. CONCLUSIONS

We have studied the partial-wave content of the $\pi^+\omega$ system produced in reaction $\pi^+ \to \pi^+\omega p$ at 7.1 GeV/c for $\pi^+\omega$ invariant mass between threshold and 1.48 GeV. We have been able to ascertain that the B meson is unlikely to be a 2^+ state; the fit is marginal and the ρ_{22} is large. With our data it is not possible to prove rigorously that the B meson is not a 2^- state, but the solution we found requires that the B have $|F/P| = 0.44 \pm 0.18$, a situation which is unlikely to occur near the threshold of a $\pi\omega$ system. In addition the 2^- state would have to be produced strongly aligned with the helicity direction. These various aspects make us feel that this solution is an artificial one and unsatisfactory.

Our best solution shows the B meson to be a 1^+ state riding over a smooth background consisting of a 1^- state and possibly a 0^- state. The 0^- background is small and consistent with zero, while the 1^- is quite large above 1.28 GeV. We have investigated the behavior of each J^P state as a function of t'. We find that the 1^+ state is peaked at low t' with no apparent dip in the forward region. From examination of the density matrices of the 1^+ state, we conclude that this state

TABLE VI. Fits as a function of t'; 5 degrees of freedom.

Moments	$0<t'<0.1$ $(\mathrm{GeV}/c)^2$ Experiment	$1^+1^-0^-$	$0.1<t'<0.4$ $(\mathrm{GeV}/c)^2$ Experiment	$1^+1^-0^-$	$0.4<t'<1.0$ $(\mathrm{GeV}/c)^2$ Experiment	$1^+1^-0^-$
$H(0000)$	459 ± 27		619 ± 31		367 ± 25	
$H(0020)$	−20 ± 13	−6	−19 ± 15	−25	4 ± 13	4
$H(0021)$	−12 ± 8	−5	6 ± 10	−8	9 ± 8	−8
$H(0022)$	−18 ± 8	−11	4 ± 9	0	0 ± 7	3
$5H(2000)$	−331 ± 57	−325	−222 ± 69	−277	−30 ± 57	−94
$5H(2020)$	15 ± 29	21	82 ± 36	57	44 ± 30	1
$5H(2021)$	−7 ± 17	16	51 ± 22	17	55 ± 18	18
$5H(2022)$	23 ± 16	23	8 ± 18	14	30 ± 16	7
$5H(2120)$	8 ± 18	26	54 ± 21	51	−11 ± 17	9
$5H(2121)$	23 ± 13	19	24 ± 16	15	25 ± 14	17
$5H(2122)$	8 ± 12	19	37 ± 14	22	0 ± 11	17
$5H(2220)$	64 ± 19	52	61 ± 21	62	38 ± 17	36
$5H(2221)$	39 ± 14	36	10 ± 15	16	16 ± 12	24
$5H(2222)$	25 ± 16	18	53 ± 18	59	56 ± 14	53
	$\chi^2 = 9.2$ CL = 10%		$\chi^2 = 6.8$ CL = 23%		$\chi^2 = 16.7$ CL = 0.5%	

TABLE VII. Fits as a function of t' for mass range 1.08–1.38 GeV.

t' [(GeV/c)^2]	χ^2 (CL)	0^-	1^+			1^-			
		No. of events	ρ_{11}	ρ_{1-1}	Reρ_{10}	No. of events	ρ_{11}	ρ_{1-1}	Reρ_{10}
0–0.1	9.2 (10%)	2 ± 22	0.23 ± 0.05	−0.19 ± 0.07	0.13 ± 0.05	185 ± 83	0.36 ± 0.06	−0.10 ± 0.10	−0.03 ± 0.06
0.1–0.4	6.8 (23%)	45 ± 27	0.21 ± 0.03	−0.13 ± 0.05	0.06 ± 0.04	130^{+120}_{-80}	0.24 ± 0.05	0.24 ± 0.19	0.06 ± 0.09
0.4–1	16.7 (0.5%)	57 ± 25	0.29 ± 0.05	−0.20 ± 0.10	0.15 ± 0.08	91^{+100}_{-60}	0.47 ± 0.11	0.38 ± 0.30	0.05 ± 0.13

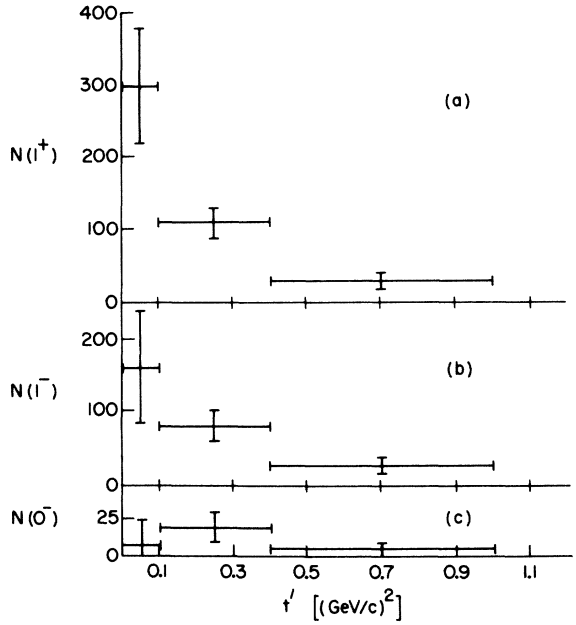

FIG. 7. Number of events in each J^P state [$N(J^P)$] as function of t' [for $1.08 < M(\pi^+\omega) < 1.38$ GeV] found by a fit to the data assuming that only 1^+, 1^-, and 0^- waves are significant.

is produced mainly via natural-parity exchange process; the most likely candidate is, of course, ω exchange.

Our conclusions are in general agreement with a recent independent analysis of the B meson produced in $\pi^- p$ interactions in which interference effects have also been taken into account.[4]

ACKNOWLEDGMENTS

We thank the Stanford Linear Accelerator 82-in. Bubble Chamber Group for their assistance in

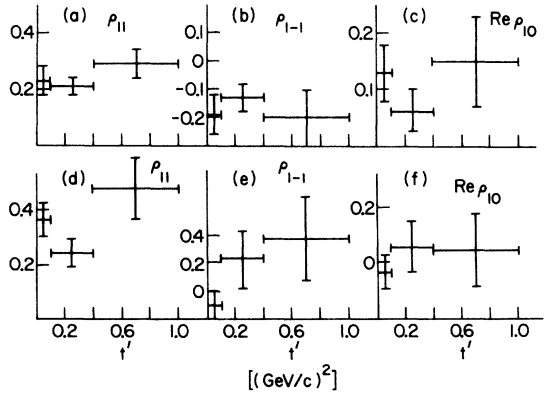

FIG. 8. (a)–(c) Density matrix as function of t' for 1^+ state [$1.08 < M(\pi^+\omega) < 1.38$ GeV] found by a fit to the data. (d)–(f) Same as (a)–(c) for 1^- state.

data gathering, and the LBL Group A Scanning and Measuring Group for their help in data reduction. We also thank Dr. R. Field for comments on production processes. It is with pleasure that two of us (S.U.C. and S.D.P.) acknowledge the encouragement of Dr. N. P. Samios during the course of this work.

APPENDIX

1. Interference moments

A $\pi\omega$ system with subsequent ω decay into three π's can be described by a set of four angles: the angles $\Omega = (\theta, \phi)$ describe the ω direction in the B rest frame, with the B direction as the z axis and the normal to the production plane as the y axis in the c.m frame; the angles $\Omega_1 = (\beta, \alpha)$ describe the normal to the ω decay plane, with the ω direction as the z' axis and the y' axis along $\vec{z}\times\vec{z}'$ in the B rest frame. The joint angular distribution in Ω and Ω_1 can be expanded in terms of a product of two D functions,[5] viz.

$$I(\Omega, \Omega_1) = \sum_{LMlm} \left(\frac{2l+1}{4\pi}\right)\left(\frac{2L+1}{4\pi}\right) H(lmLM) \times D^{L*}_{Mm}(\phi, \theta, 0)\, D^{l*}_{m0}(\alpha, \beta, 0), \quad \text{(A1)}$$

with $H(0000) = 1$ so that the over-all normalization is given by

$$\int I(\Omega, \Omega_1) d\Omega\, d\Omega_1 = 1. \quad \text{(A2)}$$

The moments $H(lmLM)$ are the experimentally measurable quantities given by

$$H(lmLM) = \langle D^{L}_{Mm}(\phi, \theta, 0) D^{l}_{m0}(\alpha, \beta, 0)\rangle. \quad \text{(A3)}$$

The moments $H(lmLM)$ depend of course on the production and decay parameters of the $\pi\omega$ system, i.e., the spin density matrix and decay helicity amplitude of each spin-parity state as well as interference effects among differerent spin-parity states. In order to exhibit explicitly the dependence of $H(lmLM)$ on these parameters, let us first break up H's into a sum of individual H's corresponding to each of the spin-parity states and their interferences; thus

$$H(lmLM) = \sum_{ij} H_{ij}(lmLM). \quad \text{(A4)}$$

Here the summation indices i and j denote different spin-parity states, i.e., $i = \{J_i, \eta_i\}$ and $j = \{J_j, \eta_j\}$, where J_i (η_i) stands for any given spin (intrinsic parity). The summation includes not only those coming from pure spin-parity states $[H_{ii}(lmLM)]$, but also interference terms $[H_{ij}(lmLM)$ and $H_{ji}(lmLM)$ for $i \neq j]$.

Each individual H_{ij} can be expressed as a product of three factors which depend on the production of the $\pi\omega$ system, the decay of the system into two-particle states of $\pi + \omega$, and the decay of the ω into 3 π's, respectively,

$$H_{ij}(lmLM) = t^{ij*}_{LM} f^{ij}_{Llm}(S0l0|S0), \quad \text{(A5)}$$

where S denotes the ω spin, i.e., $S = 1$. We emphasize that this formula is true only if the 3π system is in a 1^- state. The third factor here is the usual Clebsch-Gordan coefficient which has to do with the ω decay, and the first factor is the generalized multipole parameter which depends entirely on the production of the $\pi\omega$ system, viz.

$$t^{ij*}_{LM} = \left(\frac{2J_j+1}{2J_i+1}\right)^{1/2} \sum_{\Lambda\Lambda'} \rho^{ij}_{\Lambda\Lambda'}(J_j\Lambda' LM|J_i\Lambda), \quad \text{(A6)}$$

where $\rho^{ij}_{\Lambda\Lambda'}$ is the density-matrix element describing the interference between spin-parity states i and j (this reduces to ordinary spin density-matrix element for $i = j$) and Λ (Λ') is the helicity of the $\pi\omega$ system in the spin-parity states i (j). The over-all normalization condition $H(0000) = 1$ implies that

$$\sum_i \sum_\Lambda \rho^{ii}_{\Lambda\Lambda} = 1 \quad \text{(A7)}$$

The second factor in (A5) which describes decay of the $\pi\omega$ system into $\pi + \omega$ can be written as

$$f^{ij}_{Llm} = \sum_{\lambda\lambda'} F^i_\lambda F^{j*}_{\lambda'}(J_j\lambda' Lm|J_i\lambda)(S\lambda' lm|S\lambda), \quad \text{(A8)}$$

where S (λ or λ') is the ω spin (helicity) ($S = 1$), and F^i_λ is the decay helicity amplitude for the spin-parity state i, normalized

$$\sum_\lambda |F^i_\lambda|^2 = 1. \quad \text{(A9)}$$

Next, we shall give symmetry relations coming from parity conservation and time-reversal invariance. Parity conservation in the production and decay of the $\pi\omega$ system leads respectively to

$$\rho^{ij}_{\Lambda\Lambda'} = \eta_i\eta_j(-1)^{J_i-J_j}(-1)^{\Lambda-\Lambda'}\rho^{ij}_{-\Lambda-\Lambda'}, \quad \text{(A10)}$$

$$F^i_\lambda = \epsilon_i F^i_{-\lambda}, \quad \epsilon_i = \eta_i(-1)^{J_i-1}. \quad \text{(A11)}$$

Additional constraints on F's can be obtained from the following assumptions. Consider $\pi\omega \to \pi\omega$ scattering in a particular spin-parity state in the s channel; assume for this process that the scattering amplitude factorizes. Then, it can be shown that time-reversal invariance applied to the scattering process implies[6]

$$F^i_\lambda F^{i*}_{\lambda'} = \text{real} \quad \text{(A12)}$$

so that the phase of F^i_λ for a given spin-parity state i is independent of λ. The above assumption is certainly true, if a single resonance saturates the unitarity limit at a given energy.

The relation (A10) implies that the multipole parameters (A6) should obey the symmetry

$$t^{ij}_{LM} = \eta_i \eta_j (-1)^{L+M} t^{ij}_{L-M}, \tag{A13}$$

while Eq. (A11) imposes on the quantity (A8) the following symmetry:

$$f^{ij}_{Llm} = \eta_i \eta_j (-1)^{l+L} f^{ij}_{Ll-m}. \tag{A14}$$

We shall give one more relation which is particularly useful for a pure spin-parity state. It comes from the fact that the density-matrix element may be considered a scalar product in a complex vector space where the vectors are the production amplitudes (of the $\pi\omega$ system), which leads to the following symmetry:

$$\rho^{ij}_{\Lambda\Lambda'} = \rho^{ji*}_{\Lambda'\Lambda} \tag{A15}$$

so that the density submatrix for $i=j$ is Hermitian This in turn implies

$$t^{ij}_{LM} = \left(\frac{2J_j+1}{2J_i+1}\right)^{1/2} (-1)^{J_j-J_i}(-1)^M t^{ji*}_{L-M}. \tag{A16}$$

Combining this with Eq. (A13), one obtains

$$t^{ij}_{LM} = \left(\frac{2J_j+1}{2J_i+1}\right)^{1/2} \eta_i \eta_j (-1)^{J_j-J_i}(-1)^L t^{ji*}_{LM}. \tag{A17}$$

Note that for a pure spin-parity state $(i=j)$ t^{ii}_{LM} is purely real (imaginary) for $L=$ even (odd). For completeness, we give at this point a symmetry involving interchange of i and j in (A8):

$$f^{ij}_{Llm} = \left(\frac{2J_i+1}{2J_j+1}\right)^{1/2} (-1)^{J_i-J_j} f^{ji*}_{Ll-m}. \tag{A18}$$

Finally, we emphasize that symmetries (A13) and (A14) apply equally well to $H_{ij}(lmLM)$, since it is a product of the quantities given in (A13) and (A14) [see Eq. (A5)]. Thus (A13) and (A14) give, respectively,

$$H_{ij}(lmLM) = \eta_i \eta_j (-1)^{L+M} H_{ij}(lmL-M), \tag{A19}$$

$$H_{ij}(lmLM) = \eta_i \eta_j (-1)^{l+L} H_{ij}(l-mLM). \tag{A20}$$

Symmetry in $H_{ij}(lmLM)$ under interchange of i and j can be obtained by combining (A16) and (A18), viz.

$$H_{ij}(lmLM) = (-1)^M H^*_{ji}(l-mL-M). \tag{A21}$$

Use of relations (A19) and (A20) in (A21) gives

$$H_{ij}(lmLM) = (-1)^l H^*_{ji}(lmLM). \tag{A22}$$

This constraint ensures that the angular distribution I is real. Note that l is even (0 or 2, since $S=1$) owing to the Clebsch-Gordan coefficient appearing in (A5); this indicates that $H_{ij}(lmLM)$ for $i=j$ is real.

We are now ready to discuss the symmetries in the joint angular distribution $I(\Omega,\Omega_1)$ due to the symmetries in $H_{ij}(lmLM)$ exhibited in the previous paragraphs. For this purpose, let us first break up the angular distribution in (A1) into those corresponding to each spin-parity state and their interferences, viz.

$$I(\Omega,\Omega_1) = \sum_{ij} I_{ij}(\Omega,\Omega_1), \tag{A23}$$

where

$$I_{ij}(\Omega,\Omega_1) = \sum_{LMlm} \left(\frac{2l+1}{4\pi}\right)\left(\frac{2L+1}{4\pi}\right) H_{ij}(lmLM) \times D^{L*}_{Mm}(\phi,\theta,0) D^{l*}_{m0}(\alpha,\beta,0). \tag{A24}$$

Parity conservation in the ω decay implies that l is even (0 or 2); this in turn leads to the following symmetry in the angular distribution:

$$I_{ij}(\Omega,\Omega_1) = I_{ij}(\theta,\phi,\pi-\beta,\pi+\alpha). \tag{A25}$$

This of course has a simple geometrical interpretation. It says that the angular distribution does not change when the direction of the normal to the ω-decay plane is reversed while all other directions are held fixed.

Parity conservation in the decay of the $\pi\omega$ system into $\pi+\omega$ can be derived using relations (A20) and (A24). We find

$$I_{ij}(\Omega,\Omega_1) = \eta_i \eta_j I_{ij}(\pi-\theta,\ \pi+\phi,\ \pi-\beta,\ -\alpha). \tag{A26a}$$

The over-all angular distribution should satisfy the symmetry in (A26a) if the opposite-parity interference effects are absent (i.e., $\eta_i = \eta_j$ for all i and j). Geometrical interpretation of the right-hand side of (A26a) is that the direction of all the momenta in the $\pi\omega$ system (including those of the ω decay) are reversed, while those of the production process are held fixed. Note that reversal of the ω direction affects both the angles Ω and Ω_1; this is due to the fact that the helicity frame has been chosen to describe the ω-decay process.

Parity conservation in the production of the $\pi\omega$ system implies from (A19) and (A24)

$$I_{ij}(\Omega,\Omega_1) = \eta_i \eta_j I_{ij}(\pi-\theta,\ \pi-\phi,\ \beta,\ \pi+\alpha). \tag{A26b}$$

Again, in the absence of opposite-parity interference, (A26b) represents a symmetry in the over-all angular distribution. Angular transformations given in (A26b) correspond to reversing all the vectors involved in the production process

while those of the $\pi\omega$ decay as well as the ω decay are held fixed (this corresponds to reversing the directions of x and z axes defining the $\pi\omega$ rest system while the y axis is held constant, since the y axis is defined to be along the production normal, a pseudovector).

By combining (A26a) and (A26b), we arrive at a general symmetry relation independent of intrinsic parities:

$$I_{ij}(\Omega, \Omega_1) = I_{ij}(\theta, -\phi, \pi - \beta, \pi - \alpha). \tag{A27}$$

The transformation implied here is that of reversing the directions of all the momenta involved in the production and decay of a $\pi\omega$ system; the symmetry is of course general and cannot depend on the parities. An equivalent way of viewing the transformation is by reflection of all the momenta through the production plane.

We see therefore that there exist two independent symmetry relations (A25) and (A27) that have to be satisfied from parity conservation regardless of interference effects among different spin-parity states.

It is instructive to rewrite the angular distribution (A24) by imposing the parity-conservation conditions for both production and decay of the $\pi\omega$ system, i.e., (A19), (A20), (A22), and l = even:

$$I_{ij}(\Omega, \Omega_1) + I_{ji}(\Omega, \Omega_1) = \sum_{lL} \sum_{m\geq 0; M\geq 0} \left(\frac{2l+1}{4\pi}\right)\left(\frac{2L+1}{4\pi}\right)(2-\delta_{m0})(2-\delta_{M0})[2\,\mathrm{Re}H_{ij}(lmLM)]\,{}^{ij}E^{lm}_{LM}(\Omega, \Omega_1), \tag{A28}$$

where

$${}^{ij}E^{lm}_{LM}(\Omega, \Omega_1) = \tfrac{1}{2}\,\mathrm{Re}[D^{L}_{Mm}(\phi, \theta, 0)D^{l}_{m0}(\alpha, \beta, 0) + \eta_i\eta_j(-1)^{L+M}D^{L}_{-Mm}(\phi, \theta, 0)D^{l}_{m0}(\alpha, \beta, 0)] \tag{A29a}$$

$$= \tfrac{1}{2}\,\mathrm{Re}[D^{L}_{Mm}(\phi, \theta, 0)D^{l}_{m0}(\alpha, \beta, 0) + \eta_i\eta_j(-1)^{L}D^{L}_{M-m}(\phi, \theta, 0)D^{l}_{-m0}(\alpha, \beta, 0)]. \tag{A29b}$$

This angular distribution shows that only the real part of $H_{ij}(lmLM)$ can be determined.

Angular functions (A29) indicate that experimental measurement of moments can be split up into even and odd parts (in the sense of $\eta_i\eta_j = \pm 1$):

$$\mathrm{Re}H^{(\pm)}(lmLM) = \tfrac{1}{2}\langle \mathrm{Re}[D^{L}_{Mm}(\phi, \theta, 0)D^{l}_{m0}(\alpha, \beta, 0) \pm (-1)^{L+M}D^{L}_{-Mm}(\phi, \theta, 0)D^{l}_{m0}(\alpha, \beta, 0)]\rangle \tag{A30a}$$

$$= \tfrac{1}{2}\langle \mathrm{Re}[D^{L}_{Mm}(\phi, \theta, 0)D^{l}_{m0}(\alpha, \beta, 0) \pm (-1)^{L}D^{L}_{M-m}(\phi, \theta, 0)D^{l}_{-m0}(\alpha, \beta, 0)]\rangle, \tag{A30b}$$

where

$$\mathrm{Re}H^{(\pm)}(lmLM) = \tfrac{1}{2}\sum_{ij}(1 \pm \eta_i\eta_j)\,\mathrm{Re}H_{ij}(lmLM). \tag{A31}$$

Note that the even part of H carries the terms corresponding to pure spin-parity states, i.e.,

$$\mathrm{Re}^{(\pm)}(lmLM) = \sum_i \mathrm{Re}H_{ii}(lmLM) + 2\sum_{\substack{i>j \\ \eta_i\eta_j=1}} \mathrm{Re}H_{ij}(lmLM). \tag{A32}$$

In contrast, the odd part of H depends only on in terference effects among states with $\eta_i\eta_j = -1$:

$$\mathrm{Re}H^{(-)}(lmLM) = 2\sum_{\substack{i>j \\ \eta_i\eta_j=-1}} \mathrm{Re}H_{ij}(lmLM). \tag{A33}$$

2. Pure spin-parity state

In this section we discuss certain recombinations of moments $H(lmLM)$ which are particularly useful in a spin-parity analysis, assuming that the moments corresponding to a pure spin-parity state with spin J and parity η can be isolated. We shall henceforth drop indices i and j from summations involving them in all the formulas to be written. Our purpose here has been to collect certain useful formulas for completeness; formalism of this kind has been given in full detail elsewhere.[6]

Our starting point is Eq. (A8), which can be inverted using the orthonormality of the Clebsch-Gordan coefficients to give

$$(2S+1)\,F_\lambda F^*_{\lambda'}(J\lambda' Lm|J\lambda) = \sum_l (2l+1)\,(S\lambda' lm\,|\,S\lambda)f_{lLm}. \tag{A34}$$

We can limit the above summation to even terms by adding to Eq. (A34) a similar equation with λ and λ' changed to $-\lambda'$ and $-\lambda$:

$$\tfrac{1}{2}(2S+1)[F_\lambda F^*_{\lambda'} + (-1)^{L}F^*_{\lambda}F_{\lambda'}]\,(J\lambda' Lm|J\lambda) = \sum_{l=\text{even}} (2l+1)(S\lambda' lm|\,S\lambda)f_{lLM}. \tag{A35}$$

This shows that a quantity given by

$$B_{\lambda\lambda'}(LM) = (2S+1)\, t^*_{LM}\, \tfrac{1}{2}[F_\lambda F^*_{\lambda'} + (-1)^L F^*_\lambda F_{\lambda'}] \times (J\lambda' Lm|J\lambda) \quad \text{(A36)}$$

is an experimentally measurable quantity, viz.

$$B_{\lambda\lambda'}(LM) = \sum_{l=\text{even}} (2l+1)\frac{(S\lambda' lm|S\lambda)}{(S0l0|S0)} H(lmLM). \quad \text{(A37)}$$

Note that $B_{\lambda\lambda'}(LM)$ is real, since $H(lmLM)$ is real [see (A22)]. Reality of $B_{\lambda\lambda'}(LM)$ can be shown clearly by rewriting (A36):

$$B_{\lambda\lambda'}(LM) = (2S+1)\,\mathrm{Re}t_{LM}\,\mathrm{Re}(F_\lambda F^*_{\lambda'})(J\lambda' Lm|J\lambda), \quad \text{even } L \quad \text{(A38a)}$$

$$= (2S+1)\,\mathrm{Im}t_{LM}\,\mathrm{Im}(F_\lambda F^*_{\lambda'})(J\lambda' Lm|J\lambda), \quad \text{odd } L \quad \text{(A38b)}$$

where we have used the fact that t_{LM} is real (imaginary) if L = even (odd) [see (A17)].

It turns out that $B_{\lambda\lambda'}(LM)$ is most convenient in spin-parity analysis because it exhibits clearly the constraints among H's for a given spin and parity. Relationships among $B_{\lambda\lambda'}(LM)$'s for different combinations of λ and λ' can be seen by writing them down explicitly. From (A38a), if L = even,

$$B_{00}(LM) = 3\,\mathrm{Re}t_{LM}|F_0|^2(J0L0|J0) \quad (L \geq 0), \quad \text{(A39a)}$$

$$B_{11}(LM) = 3\,\mathrm{Re}t_{LM}|F_1|^2(J0L0|J0) \times\left[1 - \frac{L(L+1)}{2J(J+1)}\right] (L \geq 0), \quad \text{(A39b)}$$

$$B_{10}(LM) = 3\,\mathrm{Re}t_{LM}\,\mathrm{Re}(F_1F_0^*)(J0L0|J0) \times\frac{1}{2}\left[\frac{L(L+1)}{J(J+1)}\right]^{1/2} (L \geq 2), \quad \text{(A39c)}$$

$$B_{1-1}(LM) = 3\,\mathrm{Re}t_{LM}(-\epsilon)|F_1|^2(J0L0|J0) \times\left[\frac{L(L+1)}{(L-1)(L+2)}\right]^{1/2} (L \geq 2) \quad \text{(A39d)}$$

From (A37), these quantities can be measured as follows:

$$B_{00}(LM) = H(00LM) + 5H(20LM), \quad \text{(A40a)}$$

$$B_{11}(LM) = H(00LM) - \tfrac{5}{2}H(20LM), \quad \text{(A40b)}$$

$$B_{10}(LM) = (\tfrac{1}{2}\sqrt{3})5H(21LM), \quad \text{(A40c)}$$

$$B_{1-1}(LM) = -(\tfrac{3}{2})^{1/2}\,5H(22LM). \quad \text{(A40d)}$$

Let us note a few salient features derivable from these relations. Decay amplitudes F_λ can be determined via

$$\frac{B_{00}(00)}{B_{11}(00)} = \frac{|F_0|^2}{|F_1|^2}. \quad \text{(A41)}$$

A straightforward way of determining spin and parity is afforded by taking the ratio of (A39b) and (A39d),

$$\frac{B_{11}(LM)}{B_{1-1}(LM)} = (-\epsilon)\left[1 - \frac{L(L+1)}{2J(J+1)}\right]\left[\frac{(L-1)(L+2)}{L(L+1)}\right]^{1/2} \quad \text{(even } L \geq 2\text{)}, \quad \text{(A42)}$$

or, by combining (A41) with (A39a) and (A39b),

$$\frac{B_{00}(00)}{B_{11}(00)}\frac{B_{11}(LM)}{B_{00}(LM)} = 1 - \frac{L(L+1)}{2J(J+1)} \quad \text{(even } L \geq 2\text{)}. \quad \text{(A43)}$$

If F_λ is assumed real (i.e., time-reversal invariance is applicable),

$$\frac{[B_{10}(LM)]^2}{B_{00}(LM)B_{11}(LM)} = \frac{1}{2}\left[\frac{L(L+1)}{2J(J+1) - L(L+1)}\right] \quad \text{(even } L \geq 2\text{)}. \quad \text{(A44)}$$

It is sometimes convenient to rewrite (A42) in the following way:

$$\Delta_{J\eta}(LM) = \left[\frac{2L(L+1)}{3(L-1)(L+2)}\right]^{1/2}[H(00LM) - \tfrac{5}{2}H(20LM)] - \epsilon\left[1 - \frac{L(L+1)}{2J(J+1)}\right]5H(22LM) \quad \text{(even } L \geq 2\text{)}. \quad \text{(A45)}$$

Note that this quantity is in general zero only for the correct spin J and parity η and is non-zero otherwise. By evaluating (A45) for each event and summing over for a given mass bin, one avoids the cumbersome burden of carrying through the statistical correlations among moments in the calculation of experimental errors.

Let us now turn to a discussion of the angular distribution for a pure spin-parity state. From (A28), we find

$$I(\Omega, \Omega_1) = \sum_{lL}\sum_{m\geq 0;\, M\geq 0}\left(\frac{2l+1}{4\pi}\right)\left(\frac{2L+1}{4\pi}\right)(2-\delta_{M0}) \times H(lmLM)E^{lm}_{LM}(\Omega, \Omega_1), \quad \text{(A46)}$$

where the E^{lm}_{LM} are the same as those given in (A29a) and (A29b) with $\eta_i = \eta_j = \eta$. We can measure the moments $H(lmLM)$ by using (A30a) and (A30b). To wit,

$$H(lmLM) = \tfrac{1}{2}\langle \mathrm{Re}[D^L_{Mm}(\phi, \theta, 0)D^l_{m0}(\alpha, \beta, 0) + (-)^{L+M}D^L_{-Mm}(\phi, \theta, 0)D^l_{m0}(\alpha, \beta, 0)]\rangle \quad \text{(A47a)}$$

$$= \tfrac{1}{2}\langle \mathrm{Re}[D^L_{Mm}(\phi, \theta, 0)D^l_{m0}(\alpha, \beta, 0) + (-)^L D^L_{M-m}(\phi, \theta, 0)D^l_{-m0}(\alpha, \beta, 0)]\rangle. \quad \text{(A47b)}$$

Evaluation of H's by these formulas instead of (A3) should result in general in smaller statistical errors, since we have combined in (A47) two statistically independent moments that are theoretically equivalent from parity conservation.

---

*Work supported by the U. S. Atomic Energy Commission.

†Present address: Computation Group 88, Stanford Linear Accelerator Center, Stanford, California 94305.

‡Present address: Lawrence Livermore Laboratory, Livermore, California 94550.

§Present address: Physics Department, University of Massachusetts, Amherst, Massachusetts 01002.

[1]S. U. Chung *et al.*, Phys. Lett. 47B, 526 (1973).

[2]G. Ascoli *et al.*, Phys. Rev. Lett. 20, 1411 (1968); A. Werbrouck *et al.*, Nuovo Cimento 4, 1267 (1970); P. Frenkiel *et al.*, Nucl. Phys. B47, 61 (1972); U. Karshon *et al.*, Phys. Rev. D 10, 3608 (1974). For a review of previous spin-parity analysis of the B meson see paper by S. U. Chung, in *Experimental Meson Spectroscopy–1974*, proceedings of the International Conference on Experimental Meson Spectroscopy, Boston, 1974, edited by D. A. Garelick (A. I. P. New York, 1974).

[3]For experimental details on this final state see paper by R. L. Ott, Ph.D. thesis, LBL Report No. LBL-1547, 1972 (unpublished).

[4]V. Chaloupka *et al.*, Phys. Lett. 51B, 407 (1974).

[5]We use the D functions as defined by M. E. Rose, *Elementary Theory of Angular Momentum* (Wiley, New York, 1957).

[6]See, for example, S. U. Chung, CERN Report No. CERN 71-8, 1971 (unpublished).